ELSEVIER

Remote Sensing of Environment 75 (2001) 324–334

Remote Sensing of Environment

www.elsevier.com/locate/rse

The use of multiscale remote sensing imagery to derive regional estimates of forest growth capacity using 3-PGS

N.C. Coops[a,*], R.H. Waring[b]

[a]CSIRO Forestry and Forest Products, Melbourne, Australia
[b]Oregon State University, College of Forestry, Corvallis, OR, USA

Received 28 February 2000; accepted 5 August 2000

Abstract

A number of process models now exist that estimate carbon and water vapor exchange across a broad array of vegetation. Many of these models can be driven with information derived from satellite sensors. In particular, a large number use the normalized difference vegetation index to infer spatial and temporal shifts in the fraction of visible light intercepted ($f\phi_{p.a}$) by vegetation. We utilized a simplified process model (Physiological Principles Predicting Growth from Satellites), initialized with Advanced Very High Resolution Radiometer normalized difference vegetation index-derived estimates of $f\phi_{p.a}$, to estimate at monthly time steps photosynthesis, respiration, and aboveground growth of forest vegetation within a 54,000 km^2 region in southwestern Oregon. We had data available from 755 permanent survey plots to provide an independent estimate of forest growth capacity. In addition, we took advantage of a satellite-derived classification of 14 major forest types to investigate the extent that generalizations might be made about their respective productive capacities. From weather stations and statewide soil surveys, we extrapolated and transformed these sources of data into those required to drive the model (solar radiation, temperature extremes, vapor pressure deficit, and precipitation) and initialize conditions (soil water holding capacity and soil fertility). Within the mountainous region we found considerable variation existed within each 1-km^2 pixel centered on each of the survey plots. Even by excluding comparisons where local variation was high, model predictions of forest growth compared poorly with those estimated from ground survey ($r^2 = 0.4$). This variation was only partly attributed to variation in canopy $f\phi_{p.a}$. Local variation in climate and soils played an equal if not greater role. When the sample plots were stratified into 14 broad forest types, within which growth potential varied similarly (coefficient of variation for each of the 14 types averaged 6%), a good relation between predicted and measured forest growth capacity across all types resulted ($r^2 = 0.82$, $P \leqslant 0.01$, SE = 1.2 m^3 ha^{-1}yr^{-1}). The implications of these analyses suggest that: (1) models should be rigorously tested before applying across landscapes; (2) accuracy in locating plots and in extrapolating data limits spatial resolution; (3) soil surveys in mountainous regions are inaccurate and difficult to interpret; (4) mapped vegetation classifications provide a useful level of stratification; and (5) remotely sensed estimates of canopy nitrogen status and biomass increment and canopy nitrogen status are needed to improve and validate regional assessment of growth. Crown Copyright © 2001 Published by Elsevier Science Ireland Ltd. All rights reserved.

1. Introduction

Remote sensing instruments and techniques to infer climatic and surface conditions have continued to improve (Milne & Cohen, 1999) to the extent that some terrestrial ecosystem models have recently been driven almost entirely with satellite-derived information (Prince & Goward, 1995). Typical input variables relevant to processes with terrestrial models include land cover type (as influenced by natural factors as well as human use), leaf area index (L), the fraction of incoming photosynthetically active radiation that is absorbed by the canopy ($f\phi_{p.a}$), and other leaf structural and chemical attributes such as specific leaf area (SLA) and percent of nitrogen (Matson, Johnson, Billow, Miller, & Pu 1994; Smith & Curran, 1995).

Satellite remote sensing has proved effective for the purpose of mapping cover types, using either classification of multispectral data at a single point in time for relatively small areas at fine spatial resolution (Bauer, Burk, Ek, Ahern, & Queen, 1994; Woodcock et al., 1994) or multi-temporal data for large areas at a relatively coarse spatial resolution (Loveland, Merchant, Ohlen, & Brown, 1991;

* Corresponding author. CSIRO Forestry and Forest Products, Private Bag 10, Clayton South, Melbourne 3169, Australia.
E-mail address: n.coops@ffp.csiro.au (N.C. Coops).

0034-4257/00/$ – see front matter Crown Copyright © 2001 Published by Elsevier Science Ireland Ltd. All rights reserved.
PII: S0034-4257(00)00176-0

Prince & Goward, 1995; Running et al., 1994). The ability to resolve successional stages (Cohen, Spies, & Fiorella, 1995) and land use change (Moran, Brondizio, Mausel, & Wu, 1994), as well as broad biome type (Nemani, Running, & Pielke, 1996), is an important consideration with respect to parametizing ecosystem models (Reich, Turner, & Bolstad, 1999).

Validation of these regional and global data products is crucial, however, to establish the accuracy of the predictions and to assure that predictive algorithms continue to improve for applications (Cohen & Justice, 1999). To date, confidence in regional and global scale models is severely limited by the lack of adequate ground-based validation. Currently a number of research programs are attempting to develop protocols and data scaling issues to lead to a better understanding of these databases and products, such as the BigFoot project (Cohen & Justice, 1999) developed for verification of the Earth Observation System (EOS) Moderate Resolution Imaging Spectro-radiometer (MODIS) (Running et al., 1994).

Validation of regional predictions is particularly challenging in mountainous landscapes where native forests dominate and there is considerable complexity in vegetation, soils, and climate. In such landscapes many crucial assumptions are made when relating field measurements to the grid-cell predictions associated with remote sensing (Box, Holben, & Kalb, 1989; White & Running, 1994). Assessment of accuracy is virtually impossible without comparing estimates obtained from field plots and from remotely sensed imagery (Milne & Cohen, 1999; Waring & Running, 1998).

As part of a regional study in southwestern Oregon, we demonstrated that a general forest growth model [Physiological Principles Predicting Growth from Satellites (3-PGS)], initialized with satellite-derived estimates of canopy light interception ($f\phi_{p.a}$), could predict the growth capacity at 18 research sites representing a wide range of forest types ($r^2 = 0.76$ with an SE of 0.8 $m^3\ ha^{-1}yr^{-1}$, significant at $P < 0.01$) (Coops & Waring, 2000). In addition, the process model correctly differentiated rates of soil water depletion with considerable accuracy ($r^2 = 0.78$). Indirectly, the analysis supported the assumption that minimum/maximum temperature and precipitation data, available from many weather stations, could be extrapolated to 200-m resolution and transformed into a complete set of climatic variables required to drive the process model: solar radiation, vapor pressure deficits, precipitation, and mean and extreme temperatures. Moreover, by working with mean monthly meteorological data averaged over 30 years, we demonstrated that general trends in growth and soil water depletion could be predicted across the region without requiring more detailed weather data.

With confidence in the 3-PGS model and in our ability to extrapolate and transform climatic data, we expand the approach in this paper to the entire 54,000 km^2 area in southwestern Oregon. At this expanded scale, we rely on a sampling grid of permanent inventory plots established and

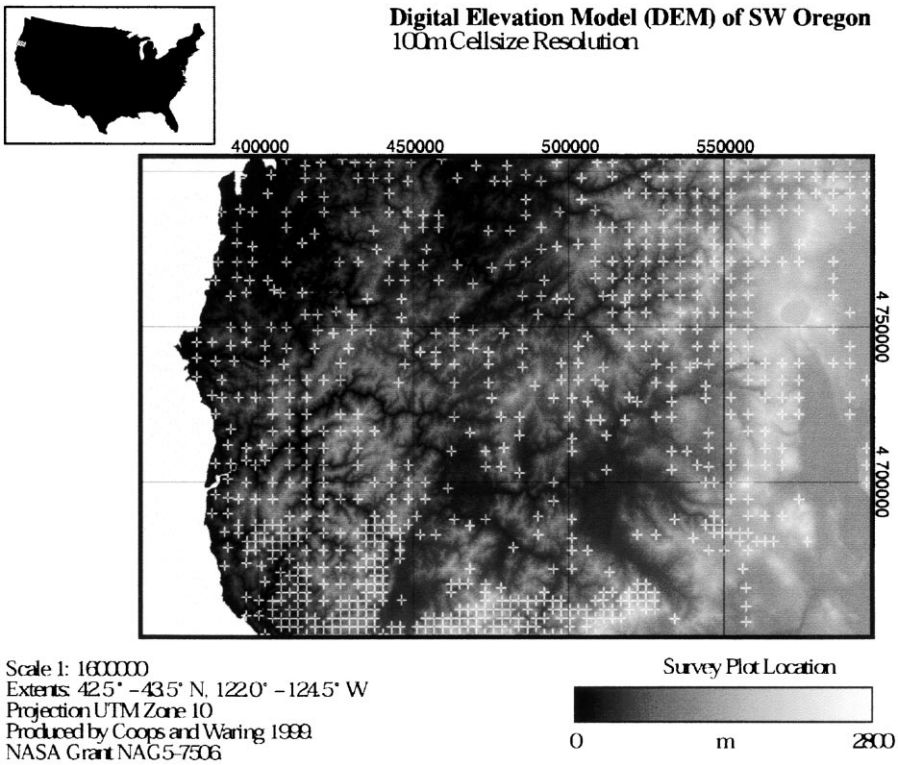

Fig. 1. Digital elevation model of the study area overlaid with forest plot locations.

monitored by the U.S. Forest Service and Bureau of Land Management (Fig. 1). From this widely distributed grid of sample points we tested the sensitivity of the modeling approach to (a) 30-m Landsat Thematic Mapper (TM) vs. a 1-km^2 Advanced Very High Resolution Radiometer (AVHRR) satellite-derived estimates of $f\phi_{p.a,}$ (b) the quality of data available on soils, and (c) the possible advantages of stratifying the landscape into a number of predefined vegetation types (Kagan & Caicco, 1996).

2. Methods

2.1. The study area

The region of interest in southwestern Oregon covers an area of 54,000 km^2 (Lat. 43° N, Long. 123° W) and contains three distinct mountain ranges: a coastal range, composed mainly of sedimentary rock; the Cascades, composed mainly of basic igneous rocks; and the Siskiyou Mountains, composed of diverse parent materials, dating back to the Silurian, more than 320 million years BP (Dahlgren, 1994; Waring, 1969). Annual precipitation varies across the region, with more than 2,500 mm recorded in the coast range and at higher elevations inland to less than 500 mm in interior valleys. In general, the area is much drier than typical of the rest of the Douglas-fir region in the Pacific Northwest (Whittaker, 1961).

2.2. Plot data

The United States Forest Service (USFS) and the Bureau of Land Management (BLM) have a number of programs to determine the extent, condition, and volume of timber on private and public lands. Three sets of plots were used in this analysis: Forest Inventory and Analysis (FIA) plots located on private land and the Current Vegetation Surveys (CVS) maintained separately by the USFS and by the BLM plots. All inventories begins with the interpretation of aerial photography to determine forest type, volume per unit area, stand size, density, and age class. Ground plots are then distributed to be representative of 1 acre (0.40 ha), using either fixed or variable radius (prism) sampling procedures. As a matter of policy, plots located on private land are shifted within 200 m of their assumed true location. As all plot positions were not located using Global Positioning System (GPS) technology, an Arc/Info Geographic Information System (GIS) search technique was used to ensure that the terrain attributes recorded at each plot (elevation, slope, and aspect) corresponded to similar attributes extracted from the Digital Elevation Model (DEM). The automated search procedure was developed whereby the initial location of each plot was shifted if necessary within specified bounds to give closer agreement with field estimates of aspect and slope (Coops, 2000). Specifically, the search routine sequentially identifies the nearest 100-m resolution cell within a search radius of five cells in which differences are within $\pm 22.5^{o}$ of aspect, $\pm 20\%$ of slope, and in closest possible agreement with elevation.

At each plot, data were acquired at 10-year intervals on standing volume, age, and height of dominant and codominant trees by species. We pooled the height and age information, regardless of species, and estimated the site index (height at age 100) for coast-range Douglas-fir from a standard yield table (McArdle, 1961). The yield table gave values on maximum periodic mean annual increment (PAI) against which values generated from the 3-PGS model could be compared. Douglas-fir production is correlated with that of other species; Sitka spruce yields are 20% higher and those of ponderosa pine are 20% lower with equivalent site indices (Hann & Scrivani, 1987). A total of 755 plots were available for analysis, 492 of which were located on public lands.

2.3. Regional vegetation type map

To aid in the analysis, a distribution of current vegetation was obtained from the Oregon Gap Analysis Program. The analysis was based on LANDSAT Multi-Spectral Scanner false-color infrared positive prints acquired at a scale of 1:250,000. These prints were photo-interpreted, with supplemental information provided from USFS and BLM files on composition of vegetation. A total of 69 vegetation associations were defined for the state (Kagan & Caicco, 1996) of which 14 were present in the study area. Table 1 lists the 14 major forest types with dominant tree species, number of survey plots, and mean and range in site indices.

2.4. AVHRR satellite data

Satellite-based measures of canopy properties such as L are desirable for net primary productivity (P_N) modeling because of its strong influence on canopy energy balances and rates of gas exchange. Research in the past decade has demonstrated that L can be obtained over large areas using empirical relationships with spectral vegetation indices such as the normalized difference vegetation index (NDVI) derived from satellite imagery (Begue, 1993; Spanner et al., 1994). Problems exist at low values of L due to exposed ground (van Leeuwen & Huete, 1996) and at high values of L, where spectral indices saturate (Fassnacht, Gower, MacKenzie, Nordheim, & Lillesand, 1997; Turner, Cohen, Kennedy, Fassnacht, & Brigs, 1999). Nevertheless, remote sensing, using both simple empirical relationships and more complex algorithms that employ radiation transfer models, has the ability to estimate L over large domains. Because of the saturation problem it is more logical to use a nearly linear relationship established between NDVI and the fraction of photosynthetically active radiation ($f\phi_{p.a}$) absorbed by the canopy. L can then be estimated by inverting Beer's

Table 1
Dominant Tree Composition Species 14 Broadly Defined Forest Types Found in Southwestern Oregon and Site Index Statistics Based on Coast Range Douglas-fir (McArdle 1961)

Forest Type	Species	Mean Site Index (m @ 100 years)	Min. Site Index (m)	Max Site Index (m)	SE Site Index (m)	No. of Survey Plots
1, Oregon White Oak–Ponderosa Pine	*Quercus garryana*–*Pinus ponderosa*	33	15	47	1.4	31
2, Oregon White Oak–California Oak	*Quercus garryana*–*Pinus ponderosa*	33	27	49	2.5	7
3, Sitka Spruce–Western Hemlock	*Picea sitchensis* – *Tsuga heterophylla*	34	21	49	1.3	28
4, Oregon White Oak–California Oak–Pacific Madrone	*Quercus garryana*–*Quercus kelloggii*–*Arbutus menziesii*	30	20	42	1.8	11
5, Douglas-fir–Tanoak–Pacific Madrone	*Abies concolor*–*Pseudotsuga menziesii*–*Libocedros decurrens*	26	14	44	2.0	18
6, Bigleaf Maple–Red Alder–Douglas-fir	*Acer macrophyllum*–*Alnus rubra*–*Pseudotsuga menziesii*	37	27	49	1.2	29
7, Douglas-fir	*Pseudotsuga menziesii*	34	14	54	0.6	160
8, Jeffery Pine	*Pinus jefferyi*	16	8	31	0.8	50
	Abies concolor–	31	12	55	0.5	281
9, White Fir–Douglas-fir–Incense Cedar	*Pseudotsuga menziesii*–*Libocedros decurrens*					
10, Ponderosa Pine	*Pinus ponderosa*	24	17	33	0.9	24
11, Lodgepole Pine	*Pinus contorta*	19	16	23	1.0	5
12, Mountain Hemlock–Red Fir	*Tsuga mertensiana* – *Abies magnifica* var. shastensis	25	14	42	1.2	34
13, Mountain Hemlock	*Tsuga mertensiana*	19	5	29	3.1	7
14, Red Fir	*Abies magnifica* var. shastensis	28	12	45	1.5	33

law or using more sophisticated radiative transfer models (Gower, Kucharik, & Norman, 1999).

Monthly, 1-km^3 NDVI imagery for 1995 was used to predict $f\phi_{p.a}$ from NDVI first using a linear equation

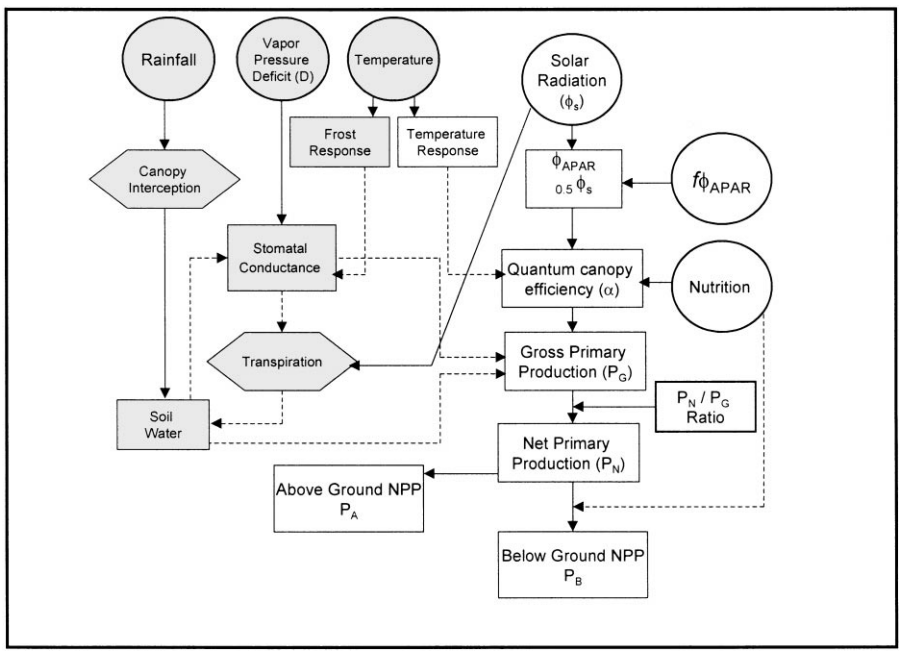

Fig. 2. Flow diagram of 3-PGS. The left hand side of the model, grey, contains components affecting predominately the hydrologic balance. Through stomatal control the hydrological components affect the carbon balance of the forest (right side of diagram).

developed by Goward, Waring, Dye, and Yang (1994) over reference sites where ground-based measurements of $f\phi_{p.a}$ were previously determined in western Oregon (Runyon, Waring, Goward & Welles, 1994). Because data were acquired for a different year, it was necessary to modify the slope of the relationship to match the original ground-based data [see Eq. (1)].

$$f\phi_{p.a} = 1.27(\text{NDVI}) - 0.03. \quad (1)$$

2.5. Landsat TM satellite data

A 1995 summer Landsat TM scene was provided for the study region by Warren Cohen, USFS Forest Science Laboratory; Corvallis, Oregon. The original data was unrectified and had to be registered onto georectified images using nearest neighbor resampling. Image to image root mean square error for the study area was 25 m using 170 Ground Control Points (GCPS).

2.6. The 3-PGS model

A recently developed model (3-PGS) (Coops, Waring, & Landsberg, 1998) utilizes a number of simple relationships derived from earlier research that allow process-based calculations to estimate forest growth in terms of a few variables. The model is based on the 3-PG model of Landsberg and Waring (1997), which gives more refined estimates of growth based on species-specific allometric relations and the $-3/2$ self-thinning law. A flow diagram of 3-PGS is presented in Fig. 2.

At monthly time steps the model requires absorbed photosynthetically active radiation ($\phi_{p.a}$), estimated as 50% global solar radiation (ϕ_s), which in this paper was derived from an established empirical relationship based on average maximum and minimum temperatures (Coops, Waring, & Moncrieff 2000a). The utilized portion of $\phi_{p.a}$ ($\phi_{p.a.u}$) is obtained by reducing $\phi_{p.a}$ by an amount determined by a series of modifiers, which take values between 0 (system "shutdown") and 1 (no constraint) imposed by (a) stomatal closure, caused by high daytime atmospheric vapor pressure deficits (D); (b) soil water balance, which is the difference between total monthly rainfall, plus available soil water stored from the previous month, and transpiration, calculated using the Penman-Monteith equation with canopy conductance (reaching a maximum value of 0.02 ms^{-1}) modified by L of the forest and constrained by monthly estimates of D (Kelliher, Lening, Raupach, & Schulze, 1995); (c) the frequency of subfreezing temperatures ($<-2°C$); and (d) a temperature quadratic function that varies between zero and unity to reduce the photosynthetic capacity when monthly mean temperatures are suboptimal (Landsberg, Waring, & Coops, 2000). The temperature optimum for coastal Douglas-fir is about 20°C, with a minimum threshold of 0°C and a maximum of 40°C (Lewis et al., 1999). A number of general physiological parameters are required for the 3-PGS model. These are listed in Table 2 (Gholz, 1982; Landsberg, 1986; Landsberg & Waring, 1997; Lewis, Olszyk, & Tingey, 1999; Linder & Murray, 1998; Waring, 2000).

Gross photosynthesis (P_G) is calculated by multiplying $\phi_{p.a}$ by a canopy quantum efficiency coefficient (α). The maximum quantum efficiency is a function of the soil fertility, and in this study with evergreen conifers was set to vary between 1.9 and 3.8 gC MJ^{-1} $\phi_{p.a.u}$. A major simplification in both forms of the model is that autotrophic respiration (R_a) is considered a fixed fraction (0.53 ± 0.04) of P_G (Landsberg & Waring, 1997; Law et al., 1999; Waring, Landsberg, & Williams, 1998). The model partitions P_N into root and aboveground biomass. The fraction of total P_N allocated to root growth increases from 0.2 to 0.6 as the ratio $\phi_{p.a.u}/\phi_{p.a}$ decreases from 1.0 to 0.2.

Table 2
Model functions and parameters used for Douglas-fir in this study

Variable	Functions and Parameter Values	Reference
Light conversion efficiency of photosynthesis	Maximum α_c ranges from 1.9–3.8 g C MJ^{-1} $\phi_{p.a.u}$, increases linearly with soil fertility	Landsberg, 1986; Linder & Murray, 1998; Waring, 2000
Constraints of light conversion efficiency associated with temperature	T_{opt} was set at 20°C, T_{min} 0°C, and T_{max} 40°C	Lewis et al., 1999
Fraction of radiation absorbed by canopy	$1-[2.718 \exp(-0.5 \cdot L)]$	Landsberg & Waring, 1997
Stomatal response to vapor pressure deficit	$g_c = g_{cmax} \exp(-2.5 \cdot D)$	Landsberg & Waring, 1977
Wood density in stands <20 years old	400 kg m^{-3}	Gholz, 1982
Maximum leaf stomatal conductance	0.006 m s^{-1}	
Maximum canopy stomatal conductance	0.02 m s^{-1}	
	$0.8/(1+\phi_{p.a.u}/\phi_{p.a.}) * 2.5 *$ highest f_I	
Fraction of production allocated to roots, monthly	Selects the most restrictive environmental constraint (e.g., with value nearest zero); includes soil fertility	Landsberg & Waring, 1997

Symbols: L = leaf area index, m^2 m^{-2}; g_{cmax} = maximum stomatal conductance, m s^{-1}; $\phi_{p.a}$ = photosynthetically active solar radiation, MJ m^{-2} $month^{-1}$; D = monthly mean daily vapor pressure deficit, kPa; $\phi_{p.a.u}$ = photosynthetically active solar radiation utilized, MJ m^{-2} $month^{-1}$; dia. = average stem diameter, mm; T_{opt} = optimum temperature for photosynthesis; g_c = stomatal conductance, m s^{-1}.

2.7. Data for 3-PGS model

2.7.1. Climate

Mean monthly minimum and maximum temperature and precipitation surfaces of the region were obtained from the Parameter-Elevation Regressions on Independent Slopes Model (PRISM) (Daly, Neilson, & Phillips, 1994) to generate 200-m resolution grid estimates of the basic climate parameters (Coops et al., 2000b).

2.7.2. Radiation

Monthly estimates of total incoming short-wave radiation were calculated using a modeling approach detailed in Coops et al. (2000a), which allows solar radiation to be predicted across landscapes through models that first calculate the potential radiation reaching any spot of ground and then reduce the value based on the clarity (transmissivity) of the atmosphere (Bristow & Campbell, 1984; Goldberg, Klein, & Mc Cartney, 1979; Hungerford, Nemani, Running, & Coughlan, 1989). Changes in the atmospheric transmissivity are mirrored in temperature extremes recorded daily and summarized monthly at weather stations present in the study area. With a DEM we adjusted for differences in slope, aspect, and elevation as well as for variations in the fraction of diffuse and direct solar beam radiation (Buffo, Fritschen & Murphy, 1972; Garnier & Ohmura, 1968; Hungerford et al., 1989; Swift, 1976). Comparison with measured radiation data demonstrated that the modeling approach predicted both the direct and diffuse components of mean monthly incoming radiation with 93–99% accuracy. On slopes, mean monthly predictions of solar radiation account for more than 87% of the observed variation with mean errors <2 MJ m^{-2} day^{-1} (Coops et al., 2000a).

2.7.3. Soil fertility

For regional scale mapping and monitoring, the State Soil Geographic (STATSGO) database is the most appropriate because it has been compiled at a consistent scale (1:250,000) for all states. STATSGO soil data are compiled from more detailed (SSURGO) soil survey maps and information on geology, topography, climate, and vegetation, supplemented by images derived through remote sensing from satellites. Using the United States Geological Survey's (USGS) 1:250,000 scale, 1- by 2-degree quadrangle series as a map base, the soil data are digitized as line segments to comply with national guidelines and standards. Soil fertility was inferred from the STATSGO mineralogy classes, which provided broad indications of the fertility of the major soil types in the region using a lookup table. The quantum efficiency α_c was modified as a function of soil fertility based on the work of Coops and Waring (2000) and Waring (2000) with α_c increasing linearly from 1.9–3.8 gC MJ^{-1} $\phi_{p.a.u}$ as the fertility ranking increases from 0 to 1.

2.7.4. Soil water holding capacity

For each STATSGO soil series, the depth of each soil horizon and its mean available soil water capacity (θ) was computed and summed for the entire profile to provide an estimate of θ for each polygon. This vector coverage was then converted to raster format with a spatial resolution (size of the cell) of 200 m, approximately equivalent to a 1:250,000 scale. If an individual cell was composed of polygons representing more than one soil series, the dominant series was selected.

The mean values of θ from the STATSGO data set was modified to take into account fine-scale variation on the DEM using Zheng, Hunt, and Running (1996) compound topographic index (CTI) (Coops, 2000). The CTI is computed as a function of the contributing area up-slope of a central cell and the slope at that central cell on the DEM (Moore, Grayson, & Ladson, 1991). Higher values of CTI tend to be found at the lower parts of watersheds and in convergent hollow areas associated with soils of low hydraulic conductivity or areas with more gentle slope than average (Beven & Wood, 1983). Soil depth and silt and clay content tend to increase from ridge tops to the valley bottoms (Singer & Munns, 1987).

3. Simulations

The 3-PGS simulations were completed on a PC workstation using GIS software with meteorological and soil data presented at 200-m spatial resolution. Model predictions were made for 12 months from climatic data averaged over a period of 30 years. To compare predictions with ground-based measurements of site index, we extracted model predictions of maximum annual aboveground $P_{A,}$ more than 90% of which is stem and branch wood after stand closure at about age 20, and compared these with the maximum PAI given in the McArdle (1961) yield tables from field-derived estimates of site index.

4. Results

Fig. 3 compares predictions of $f\phi_{p.a}$ estimated from the single 30-m Landsat TM image and the annual maximum predicted $f\phi_{p.a}$ value predicted by the 3-PGS model from the AVHRR pathfinder data. The figure shows close agreement in the prediction of $f\phi_{p.a}$ at the two spatial resolutions when $f\phi_{p.a}$ is low; however, as the $f\phi_{p.a}$ increases, the correspondence between predictions is diminished, especially at $f\phi_{p.a}>0.7$ (i.e., 70% of radiation intercepted).

The high resolution Landsat imagery provides the capacity to discriminate plots situated in locations where climatic and soil properties vary significantly within the 1-km^2 area discerned with AVHRR imagery. The relationship between $f\phi_{p.a}$. predicted with the broad scale AVHRR imagery and the fine-scale Landsat TM imagery is presented in Fig. 3.

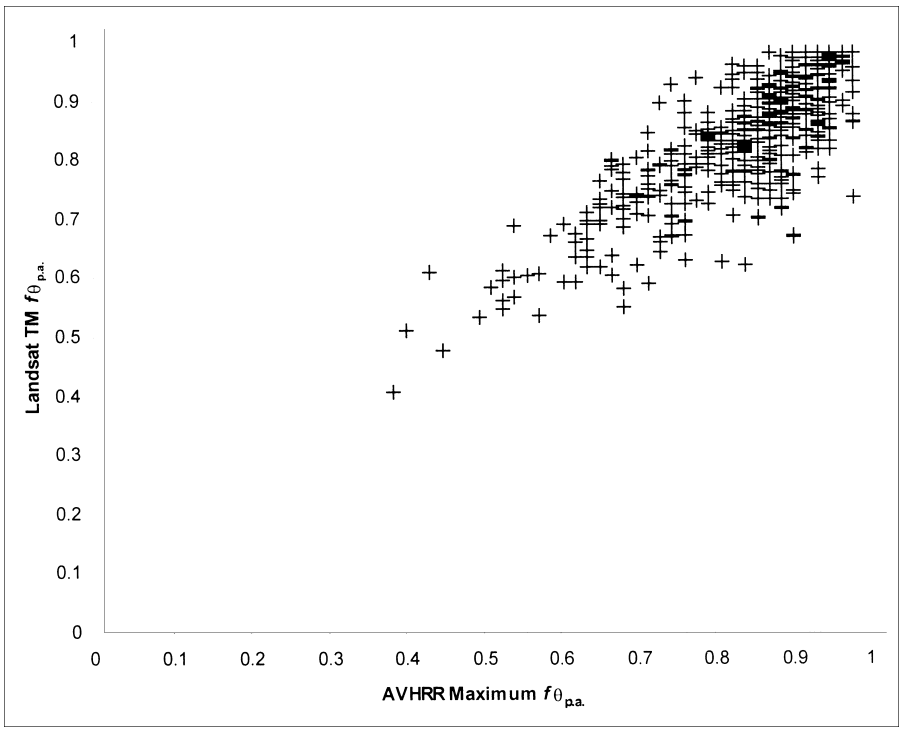

Fig. 3. Comparison of the fraction of photosynthetically active radiation absorbed by vegetation ($f\phi_{p.a}$) estimated with AVHRR and Landsat TM imagery.

Although there is considerable variation, the SE of the comparison of the AVHRR- and Landsat TM-derived $f\phi_{p.a}$ is 7% over all plots. From this figure we conclude that errors associated with estimates of $f\phi_{p.a}$ are likely not to be a major contribution to errors in modeling forest growth capacity in this study.

Interrogation of the Landsat TM-derived estimates of $f\phi_{p.a}$ within each AVHRR 1-km^2 cell indicated the maximum variation did not exceed 40% of $f\phi_{p.a}$. Figure 4 shows the relationship between the 3-PGS-predicted stemwood P_A compared to the site index maximum PAI obtained from the forest data sets where the exact plot position was assumed to

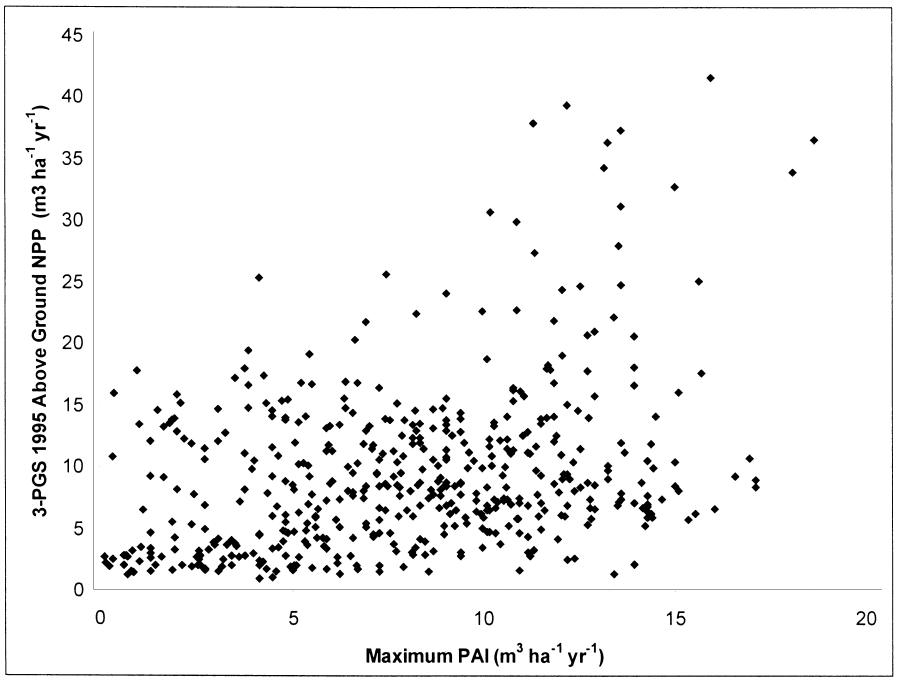

Fig. 4. At individual survey plots ($n=492$) modeled and measured maximum periodic annual increment (PAI) were poorly correlated ($r^2=0.13$).

be correct (i.e., plots on public lands). Fig. 4 indicates a very poor relationship between the two variables ($r^2 = 0.13$ although $P < 0.001$ with $n = 492$).

Based on the poor relationship in Fig. 4 and the degree of variation present within each of the 1-km AVHRR cells, we screened the 492 plot predictions of $f\phi_{p.a}$ to ensure that each 1-km^2 AVHRR pixel was homogenous (maximum variation did not exceed 20% of $f\phi_{p.a}$). Using this screening procedure, together with the slope and aspect check, only 110 plots remained for the analysis. With this more stringent selection of plots relationship between predicted and measured maximum, PAI only slightly improved ($r^2 = 0.4$). Some of this variation is no doubt associated with steep topography and local variation in soils (Waring & Youngberg, 1972).

If local variation in topography and soils cannot be adequately characterized, it is likely that they will be misrepresented, and thus lower the predictive capacity of any model. Although Landsat TM imagery may not provide a great improvement in estimates of $f\phi_{p.a}$, it is definitely better than AVHRR imagery for discerning differences in forest types. We therefore evaluated the possibility that estimates of forest growth capacity derived from 3-PGS using 1-km AVHRR imagery would show better agreement when averaged for the 14 forest types presented in Table 1. Using all of the plots, we found general agreement between mean maximum PAI values of forest productivity predicted and measured for the 14 forest types with similar SEs for both sources ($r^2 = 0.82$, $P \leqslant 0.01$, SE = 1.2 m^3 ha^{-1}yr^{-1}, $n = 14$; see Fig. 5).

The single outlier in Fig. 5 is the Coastal Rain forest type. The maximum PAI for this type is consistently overestimated by the 3-PGS model. A detailed analysis of the model predictions indicate that we probably assigned a too-high fertility rating to the coastal soil types where the sitka spruce-western hemlock dominates. As a result, the α value for this type was probably inflated, and less production was allocated to roots than probably warranted.

If this forest type is excluded from the regression, the fit is improved and is closer too the 1:1 relation ($r^2 = 0.92$, $P \leqslant 0.01$, $n = 13$). This regression can be further improved ($r^2 = 0.93$, $P \leqslant 0.01$, $n = 13$) by recognizing that pine growth is 20% less and Sitka spruce 20% more than represented by Douglas-fir yield tables (Hann & Scrivani, 1987).

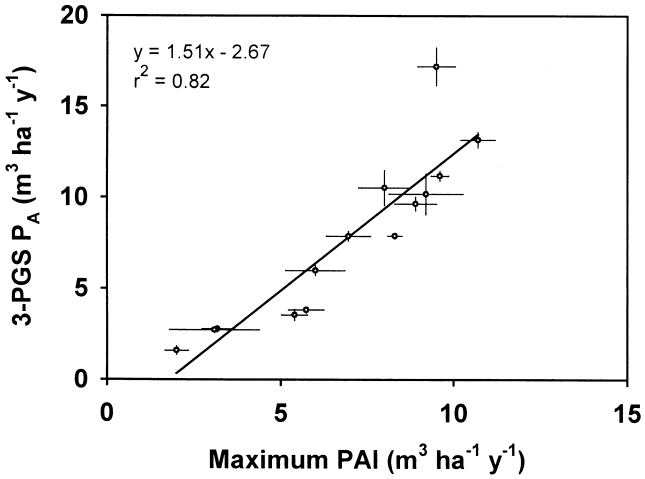

Fig. 5. Measured and predicted maximum periodic mean annual increment were highly correlated when stratified by forest types ($r^2 = 0.82$)

5. Discussion

Our decision to estimate forest growth capacity rather than actual growth greatly simplified the analysis. First, this is because determination of site index is essentially unaffected by stocking density or stand age, whereas both of these variables are required to estimate actual growth. Second, because the L of western evergreen forests is relatively stable throughout the year (Spanner et al., 1994), a single estimate of maximum NDVI obtained when deciduous plants are in full leaf during the summer is adequate to characterize the seasonal canopy light absorption ($f\phi_{p.a}$) by fully stocked evergreen forests (Franklin, Lavigne, Deuling, Wulder, & Hunt, 1997; Goward, Tucker, & Dye, 1985; Goward et al., 1994). Third, extrapolation and transformation of weather data can be accomplished with fewer errors at monthly than at daily time steps (Coops et al., 2000b). In spite of these advantages, our initial success in predicting growth capacity at individual survey sites was uninspiring, even with finer-scale estimates of NDVI provided by Landsat TM imagery. Only by recognizing the spatial distribution of major forest types and stratifying were we able to obtain general agreement between modeled and measured growth capacity.

To what extent may we attribute the problem of estimating growth capacity to the quality of data available at individual sites versus inappropriate assumptions in the model? As a prerequisite to regional analysis, we first tested the 3-PGS model and climatic extrapolation routines for 18 sites in the Siskiyou Mountains, where detailed information on seasonal trends in the availability of soil water, bioassays of soil fertility, leaf area estimates, and growth were recorded (Coops & Waring, 2000). Model predictions of seasonal water deficits and maximum periodic mean annual increment both agreed within about 20% of measured values. Considering that a 20% difference in growth capacity exists between Douglas-fir, our reference species, and other tree species in the area, these results were encouraging. In addition, we have demonstrated that the 3-PGS model and its precursor, 3-PG, apply well at other sites (Coops, 1999; Landsberg et al., 2000), including those where water vapor and CO_2 exchange were monitored continuously throughout the year to assess monthly variation in latent heat exchange and gross photosynthesis (Law, Baldocchi, & Anthoni, 1999; Waring et al., 1995). With the

objectives of estimating growth capacity of evergreen forests, the 3-PGS model seems well suited.

Alternatively, we discovered a number of problems in the quality of data available. One gains the impression from the widespread availability of DEMs that soil, topographic, and related physiographic features of landscapes are accurately mapped. We found, however, that in the mountains of southwestern Oregon, many plot locations are inaccurate (Coops, 2000). Although ground-based measurements of elevation often agree with those derived from a DEM, aspects and slopes may differ, which introduces large errors in estimates of incoming shortwave radiation. A routine was devised to shift plots to the nearest location with comparable physiography (Coops, 2000), but the relocation may result in shifts that can extend up to 430 m. In the data set available in this analysis, all survey plots on private lands were purposely shifted from their assumed "true" location by 200 m. Even when an automated relocation routine was applied, modeled and measured values of maximum PAI were in poor agreement ($r^2 = 0.4$).

Although there are problems in extrapolating climatic data in mountainous regions, we have general confidence in the approach, based on successful applications in the Siskiyou Mountains and elsewhere (Coops & Waring, 2000). We also justify averaging weather data over 30 years as appropriate for generalizing growth capacity of trees that range in age from 20 to 200 years.

The two remaining variables that may account for lack of agreement between modeled and measured growth capacity at individual survey plots are soil properties related to water storage and fertility. The estimates of available water that can be stored in the rooting zone are derived as a function of soil texture and topographic position. In general, the derived values seem reasonable (Coops, 2000; Zheng et al., 1996), although rooting depth is known to vary with species (Waring & Running, 1998). On the other hand, soil fertility is extremely difficult to interpret from soil surveys, even when mapped at fine spatial resolution because release of nutrients through decomposition and weathering vary with the environment and are affected by species composition and supplemental inputs of nutrients (Waring, 2000).

The STATSGO data set is consistent and applicable at broad geographic scales, but is clearly inadequate for local application, especially in mountainous areas. These inadequacies can be appreciated by inspecting soil type variation present within a 1-km cell (Burrough, 1986) and recognizing the difficulty of locating survey plots accurately within that matrix.

When estimates of soil fertility derived from STATSGO classification were stratified within a specified forest type, mean estimates of modeled growth capacity more closely matched those derived from survey plots (Fig. 5). In areas where we lacked independent assessment of soil fertility through bioassays (Waring and Youngburg, 1972), such as sitka spruce-western hemlock type along the Pacific coast, we observed the greatest departure between modeled and measured growth capacity. If we had complete confidence in the extrapolation of climatic conditions and assessment of $f\phi_{p.a}$, we could adjust the assessment of soil fertility to match yield predictions with those measured (Waring, 2000).

Alternately, advancements in remote sensing may offer independent measures that more adequately address the problem of interpreting soil properties and assessing growth. With finer spectral resolution in satellite-borne sensors, we recognize that it would be possible to characterize landscapes in regard to the concentration and total amount of nitrogen in canopies (Martin & Aber, 1997; Matson et al., 1994; Smith & Curran, 1995; Waring et al., 1995). Nitrogen, although not the only nutrient affecting growth, is the one most generally correlated with affecting photosynthetic capacity and the partitioning of growth (Reich, Kloeppel, Ellsworth, & Walters, 1995; Waring & Running, 1998). Similarly, lidar technology offers the potential to estimate net changes in forest biomass across landscapes with considerable accuracy (Lefsky, Harding, Cohen, Parker, & Shugart, 1999). Growth estimates, however, will still need to be stratified within broad vegetation units because sampling with lidar is intensive and therefore spatially limited.

In summary, we generalize from this analysis the following key points:

- Models should be rigorously tested before applying across landscapes.
- Accuracy in locating plots and in extrapolating data limits spatial resolution is essential.
- Soil surveys in mountainous regions are inaccurate and difficult to interpret.
- Mapped vegetation classifications provide a useful level of stratification.
- Remotely sensed estimates of canopy nitrogen status and biomass increment are needed to improve regional assessments of growth.

Acknowledgments

We wish to thank Dr. Joe Landsberg for important insights concerning the application of 3-PG. Dr. Janet Ohman (USFS, Corvallis) provided the forest data sets and useful advice. Mr. Stephen Brown (University of Montana, Missoula) prepared the DEM for analysis. Dr. Warren Cohen (USFS, Pacific NW Research Station, Corvallis) provided access to the Landsat TM imagery. This research was undertaken at Department of Forest Science, Oregon State University, Oregon while Dr Coops was on leave from CSIRO Forestry and Forest Products, Australia. Support was provided from the National Aeronautics and Space Administration (NASA), Grant NAG5-7506. Additional information on this research is available at http://www.fsl.orst.edu/bevr/.

References

Bauer, M. E., Burk, T. E., Ek, A. R., Ahern, S. C., & Queen, L. P. (1994). Satellite inventory of Minnesota forest resources. *Photogrammetric Engineering and Remote Sensing*, *60*, 287–298.

Begue, M. E. (1993). Leaf Area Index, intercepted photosynthetically active radiation, and spectral vegetation indices. A sensitivity analysis for regular clumped canopies. *Remote Sensing of Environment*, *46*, 45–59.

Beven, K. J., & Wood, E. F. (1983). Catchment geomorphology and the dynamics of runoff contributing areas. *Journal of Hydrology*, *65*, 139–158.

Box, E. O., Holben, B. N., & Kalb, V. (1989). Accuracy of the AVHRR vegetation index as a predictor of biomass, primary productivity and net CO^2 flux. *Vegetatio*, *80*, 71–89.

Bristow, K. L., & Campbell, G. S. (1984). On the relationship between incoming solar radiation and daily maximum and minimum temperature. *Agricultural and Forest Meteorology*, *31*, 159–166.

Buffo, J., Fritschen, L., and Murphy, J. (1972), *Direct Solar Radiation on Various Slopes from 0° to 60° North Latitude,* Res. Pap. PAW-142. US. Department of Agriculture Forest Service, Portland OR.

Burrough, P. A. (1986). *Principles of Geographical Information Systems for Land Resources Assessment*. Oxford: Clarendon Press.

Cohen, W. B., & Justice, C. O. (1999). Validating MODIS terrestrial ecology products: linking *in situ* and satellite measurements. *Remote Sensing of Environment*, *70*, 52–68.

Cohen, W. B., Spies, T. A., & Fiorella, M. (1995). Estimating the age and structure of forests in a multi-ownership landscape of Western Oregon, U.S.A. *International Journal of Remote Sensing*, *16*, 721–746.

Coops, N. C. (2000). Comparison of topographic and physiographic properties measured on the ground with those derived from digital elevation models. *Northwest Science*, *74* (2), 116–130.

Coops, N. C. (1999). Linking multi-resolution satellite-derived estimates of canopy photosynthetic capacity and meteorological data to assess forest productivity in a *Pinus radiata* (D. Don) stand. *Photogrammetric Engineering and Remote Sensing*, *65*, 1149–1156.

Coops, N. C., Waring, R. H., & Landsberg, J. J. (1998). Assessing forest productivity in Australia and New Zealand using a physiologically-based model driven with averaged monthly weather data and satellite derived estimates of canopy photosynthetic capacity. *Forest Ecology and Management*, *104*, 113–127.

Coops, N. C., Waring, R. H., & Moncrieff, J. (2000a). Estimating mean monthly incident solar radiation on horizontal and inclined slopes from mean monthly temperatures extremes. *Journal of Biometeorology* (in press).

Coops, N. C., Phillips, N., Waring, R. H., & Landsberg, J. J. (2000b). Prediction of solar radiation, vapor pressure deficit, and occurrence of frost from mean daily temperature extremes. *Agriculture and Forest Meteorology* (in review).

Coops, N. C., & Waring, R. H. (2000). Estimating maximum potential site productivity and site water stress of the eastern Siskiyous using 3-PGS. *Canadian Journal of Forest Research* (in review).

Daly, C., Neilson, R. P., & Phillips, D. L. (1994). A statistical-topographic model for mapping climatological precipitation over mountainous terrain. *Journal of Applied Meteorology*, *33*, 40–158.

Dahlgren, R. A. (1994). Soil acidification and nitrogen saturation from weathering of ammonium-bearing rock. *Nature*, *368*, 838–841.

Fassnacht, K. S., Gower, S. T., MacKenzie, M. D., Nordheim, E. V., & Lillesand, T. M. (1997). Estimating the leaf area index of north central Wisconsin forests using the Landsat Thematic Mapper. *Remote Sensing of Environment*, *61*, 229–245.

Franklin, S. E., Lavigne, M. B., Deuling, M. J., Wulder, M. A., & Hunt, R. Jr. (1997). Estimation of forest Leaf Area Index using remote sensing and GIS data for modelling net primary production. *International Journal of Remote Sensing*, *18*, 3459–3471.

Garnier, B. J., & Ohmura, A. (1968). A method for calculating the direct shortwave radiation income on slopes. *Journal of Applied Meteorology*, *7*, 796–800.

Gholz, H. L. (1982). Environmental limits on aboveground net primary productivity, leaf area and biomass in vegetation zones of the Pacific Northwest. *Ecology*, *63*, 469–481.

Goldberg, B., Klein, W. H., & Mc Cartney, R. D. (1979). A comparison of some simple models used to predict solar irradiance on a horizontal surface. *Solar Energy*, *23*, 81–83.

Gower, S. T., Kucharik, C. J., & Norman, J. (1999). Direct and indirect estimation of leaf area index, fAPAR and net primary production of terrestrial ecosystems. *Remote Sensing of Environment*, *70*, 29–51.

Goward, S. N., Tucker, C. J., & Dye, D. G. (1985). North American vegetation patterns observed with the NOAA-7 advanced very high resolution radiometer. *Vegetatio*, *64*, 3–14.

Goward, S. N., Waring, R. H., Dye, D. G., & Yang, J. (1994). Ecological remote sensing at OTTER: satellite macroscale observations. *Ecological Applications*, *4*, 322–343.

Hann, D. W., and Scrivani, J. A. (1987), *Dominant-Height-Growth and Site-Index Equations for Douglas-fir and Ponderosa Pine in Southwest Oregon,* Research Bulletin 59. Oregon State University, Forest Research Lab., Corvallis, Oregon.

Hungerford, R. D., Nemani, R. R., Running, S. W., and Coughlan, J. C. (1989), *MTCLIM: A Mountain Microclimate Simulation Model,* United States Department of Agriculture Research paper INT0414. Ogden, Utah.

Irwin, W. P. (1966). Geology of Klamath Mountains province. *Bulletin-California, Division of Mines and Geology*, *190*, 19–38.

Kagan, J., and Caicco, S.(1996), *Manual of Oregon Actual Vegetation,* Oregon Gap Analysis Program. U.S. Fish and Wildlife Service, Portland, OR.

Kelliher, F. M., Leuning, R., Raupach, M. R., & Schulze, E. D. (1995). Maximum conductance for evaporation from global vegetation types. *Agricultural and Forest Meteorology*, *73*, 1–16.

Landsberg, J. J. (1986). *Physiological Ecology of Forest Production*. Sydney: Academic Press.

Landsberg, J. J., & Waring, R. H. (1997). A generalized model of forest productivity using simplified concepts of radiation-use efficiency, carbon balance, and partitioning. *Forest Ecology Management*, *95*, 209–228.

Landsberg, J. J., Waring, R. H., & Coops, N. C. (2000). Performance of the forest productivity model 3-PG applied to a wide range of forest types. I. Model structure, calibration and sensitivity analysis. *Forest Ecology Management* (in review).

Law, B. E., Baldocchi, D. D., & Anthoni, P. M. (1999). Below-canopy and soil CO^2 fluxes in a ponderosa pine forest. *Agricultural and Forest Meteorology*, *94*, 171–188.

Lefsky, M. A., Harding, D., Cohen, W. B., Parker, G., & Shugart, H. H. (1999). Surface lidar remote sensing of basal area and biomass in deciduous forests of eastern Maryland, USA. *Remote Sensing of Environment*, *67*, 83–98.

Lewis, J. D., Olszyk, D., & Tingey, D. T. (1999). Seasonal patterns of photosynthetic light response in Douglas-fir seedlings subjected to elevated atmospheric CO^2 and temperature. *Tree Physiology*, *19*, 243–252.

Linder, S., & Murray, M. (1998). Do elevated CO2 concentrations and nutrients interact? In: P. G. Jarvis (Ed.), *European Forests and Global Change* (pp. 215–235). Cambridge: Cambridge Univ. Press.

Loveland, T. R., Merchant, J. W., Ohlen, D. O., & Brown, J. F. (1991). Development of a land cover characteristics database for the conterminous U.S. *Photogrammetric Engineering and Remote Sensing*, *57*, 1453–1463.

Martin, M. E., & Aber, J. D. (1997). Estimating forest canopy characteristics as inputs for models of forest carbon exchange by high spectral resolution remote sensing. In: H. L. Gholz, K. Nakane, & H. Shimoda (Eds.), *The Use of Remote Sensing in the Modelling of Forest Productivity* (pp. 61–72). Dordrecht, The Netherlands: Kluwer Academic Publishers.

Matson, P., Johnson, L., Billow, C., Miller, J., & Pu, R. (1994). Seasonal patterns and remote spectral estimation of canopy chemistry across the Oregon transect. *Ecological Applications*, *4*, 280–298.

McArdle R. E. (1961) *The Yield of Douglas-fir in the Pacific Northwest.* Tech. Bull. 201.U.S.D.A., Washington D.C.

Milne, B. T., & Cohen, W. B. (1999). Multiscale assessment of binary and continuous landcover variables for MODIS validation, mapping and modeling applications. *Remote Sensing of Environment*, *70*, 82–98.

Moore, I. D., Grayson, R. B., & Ladson, A. R. (1991). Digital terrain modelling—A review of hydrological, geomorphological and biological applications. *Hydrology Proceedings*, *5*, 3–30.

Moran, E. F., Brondizio, E., Mausel, P., & Wu, P. (1994). Integrating Amazonian vegetation, land-use and satellite data. *Bioscience*, *44*, 329–338.

Nemani, R., Running, S. W., & Pielke, R. A. (1996). Global vegetation cover changes from coarse resolution satellite data. *Journal of Geophysical Research, [Atmospheres]*, *101* (D3), 7157–7162.

Prince, S. D., & Goward, S. M. (1995). Global primary production: a remote sensing approach. *Journal of Biogeography*, *22*, 815–835.

Reich, P. B., Kloeppel, B. D., Ellsworth, D. S., & Walters, M. B. (1995). Different photosynthesis-nitrogen relations in deciduous hardwood and evergreen coniferous tree species. *Oecologia*, *104*, 24–30.

Reich, P. B., Turner, D. P., & Bolstad, P. (1999). An approach to spatially distributed modeling of net primary production (NPP) at the landscape scale and its application in validation of EOS NPP products. *Remote Sensing of Environment*, *70*, 69–81.

Running, S. W., Justice, C. O., Salomonson, V., Hall, D., Barker, J., Kaufmann, Y. J., Strahler, A. H., Huete, A. R., Muller, J.-P., Vanderbilt, V., Wan, Z. M., Teillet, P., & Carneggie, D. (1994). Terrestrial remote sensing science and algorithms planned for EOS/MODIS. *International Journal of Remote Sensing*, *15*, 3587–3620.

Runyon, J., Waring, R. H., Goward, S. N., & Welles, J. M. (1994). Environmental limits on net primary production and light-use efficiency across the Oregon transect. *Ecological Applications*, *4*, 226–237.

Singer, M. J., & Munns, D. N. (1987). *Soils: an Introduction*. New York: Macmillan Publishing Company.

Smith, G. M., & Curran, P. J. (1995). The estimation of foliar biochemical content of a slash pine canopy from AVIRIS imagery. *Canadian Journal of Remote Sensing*, *21*, 234–244.

Spanner, M. A., Johnson, L., Miller, J., McCreight, R., Freemantle, J., Runyon, J., & Gong, P. (1994). Remote sensing of seasonal leaf area index across the Oregon transect. *Ecological Applications*, *4*, 258–271.

Swift, L. W. (1976). Algorithm for solar radiation on mountain slopes. *Water Resources Research*, *121*, 108–112.

Turner, D. P., Cohen, W. B., Kennedy, R. E., Fassnacht, K. S., & Brigs, J. M. (1999). Relationship between leaf area index and Landsat TM spectral vegetation indices across three temperate zone sites. *Remote Sensing of Environment*, *70*, 52–68.

Van Leeuwen, W. J. D., & Huete, A. R. (1996). Effects of standing litter on the biophysical interpretation of plant canopies with spectral indices. *Remote Sensing of Environment*, *55*, 123–138.

Waring, R. H. (1969). Forest plants of the eastern Siskiyous: their environmental and vegetational distribution. *Northwest Science*, *43*, 1–17.

Waring, R. H. (2000). A process model analysis of environmental limitations on the growth of Sitka spruce plantations in Great Britain. *Forestry*, *75*, 65–79.

Waring, R. H., Landsberg, J. J., & Williams, M. (1998). Net primary production of forests: a constant fraction of gross primary production? *Tree Physiology*, *18*, 129–134.

Waring, R. H., Law, B. E., Goulden, M. L., Bassow, S. L., Mccreight, R. W., Wofsy, S. C., & Bazzaz, F. A. (1995). Scaling gross ecosystem production at Harvard Forest with remote sensing: a comparison of estimates from a constrained quantum-use efficiency model and eddy correlation. *Plant Cell Environment*, *18*, 1201–1213.

Waring, R. H., & Running, S. W. (1998). *Forest ecosystems: analysis at multiple scales*. San Diego, California: Academic Press.

Waring, R. H., & Youngberg, C. T. (1972). Evaluating forest sites for potential growth response of trees to fertilizer. *Northwest Science*, *46*, 67–75.

White, J. D., & Running, S. W. (1994). Testing scale dependent assumptions in regional ecosystem simulations. *Journal of Vegetation Science*, *5*, 687–702.

Whittaker, R. H. (1961). Vegetation history of the Pacific Coast States and the "central" significance of the Klamath region. *Madrofio*, *16*, 5–23.

Woodcock, C. E., Collins, J. B., Gopal, S., Jakabhazy, V. D., Li, X., Macomber, S., Ryherd, S., Harward, V. J., Levitan, J., Wu, Y., & Warbington, R. (1994). Mapping forest vegetation using Landsat TM imagery and a canopy reflectance model. *Remote Sensing of Environment*, *50*, 240–254.

Zheng, D., Hunt, E. R., & Running, S. W. (1996). Comparison of available soil water capacity estimated from topography and soil series information. *Landscape Ecology*, *11*, 3–14.